Progress In Electromagnetics Research, Vol. 141, 553–575, 2013

A NEW PARAMETER ESTIMATION METHOD FOR GTD MODEL BASED ON MODIFIED COMPRESSED SENSING

Xingwei Yan*, Jie-Min Hu, Ge Zhao, Jun Zhang, and Jianwei Wan

School of Electronic Science and Engineering, National University of Defense Technology, Changsha 410073, China

Abstract—The electromagnetic scattering mechanism of radar targets in the high-frequency domain can be characterized exactly by geometrical theory of diffraction (GTD) model. In this paper, we propose a novel parameter estimation method for GTD model based on compressed sensing. The sparse characteristic of radar echoes is analyzed, and the parameter estimation problem is converted to one of sparse signal reconstruction. Furthermore, clustering and linear least-minimum-squares algorithms are utilized to improve the accuracy of the result. Compared with several modern spectral estimation techniques, the proposed method gives a more precise estimation of the GTD model parameters, especially the scattering centers. Simulations with synthetic and measured data in an anechoic chamber confirm the effectiveness of the method.

1. INTRODUCTION

In the optical region, the electromagnetic scattering characteristics of a radar target can be regarded as coherent syntheses of electromagnetic scattering sources in several local positions. These electromagnetic scattering sources, known as scattering centers [1], are mainly generated around discontinuous parts of the target, such as edges, corners, vertexes, and inflexions. Scattering centers identify the physical locations and other relevant scattering information of the radar target, such as the type and reflection intensity of the scattering sources. The information embodied in scattering centers can be utilized

Received 20 May 2013, Accepted 29 July 2013, Scheduled 1 August 2013

* Corresponding author: Xingwei Yan (yanxingwei@nudt.edu.cn).

in target data inversion [2], interpolation or extrapolation of radar cross-section (RCS) [3], reconstruction of high-resolution range profile (HRRP) [4] and synthetic aperture radar (SAR) images [5], and radar stealthy/anti-stealthy techniques. More specifically, the extraction of scattering center parameters can enhance the detection ability of radar, and play an important role in radar target recognition [6].

Several models for the extraction of scattering centers have been established. Common scattering center models include the (undamped) exponential model [7], damped exponential model [8], and Geometrical Theory of Diffraction (GTD) model [1, 9]. Usually, the (undamped/damped) exponential model obtains a good, consistent description for traditional targets that are mainly constituted of specular scattering sources. However, as stealth technology develops, the specular scattering of stealthy objects has broadly been eliminated. Furthermore, one of the primary scattering centers of these stealthy objects is a result of edge diffraction. Unlike the damped exponential model, the GTD model is able to describe the high-frequency electromagnetic scattering of stealthy objects, such as edge diffraction, corner diffraction, point scattering, and curved surface reflection.

Traditional GTD model approaches are based on modern spectrum methods, such as the Matrix Enhancement and Matrix Pencil (MEMP) [10, 11], multiple signal classification (MUSIC) [12, 13], and Estimation of Signal Parameters via Rotational Invariance Techniques (ESPRIT) algorithms [13, 14]. These methods describe the measured scattering behavior using a two-step parametric model based on model order selection [15] and parameter estimation. The range resolution of these methods is not bandwidth limited, but is instead limited by the fitness of model order selection and the fidelity with which a particular model describes the actual scattering behavior. Moreover, their results are somewhat sensitive to signal-to-noise-ratio (SNR), and performance can degrade rapidly as the sampling rate decreases.

The recently developed field of Compressive Sensing (CS), proposed by Donoho [16] and Candés et al. [17], has attracted increasing attention in the field of radar applications. Owing to its compressed sampling and exact reconstruction ability, CS has been widely used in radar signal processing [18], such as high-resolution radar [19], Ground-Penetrating Radar (GPR) [20], through-wall radar imaging [21], SAR [22, 23], and ISAR imaging [24]. Motivated by these properties of CS theory, we propose a novel algorithm for parameter estimation in GTD models.

In the novel algorithm, the sparsity of the radar target echo model is analyzed, and a modified CS (MCS) algorithm is adopted to reconstruct the sparse parameter vectors of target scattering centers

along the range distribution. Because of measurement noise and the energy of one scattering center separating in neighboring range resolution cells, some error is introduced to the scattering center parameter of the reconstructed sparse vector. In order to reduce this error, a clustering method is used to adjust the number of scattering centers, and the least-minimum-squares method is applied to modify their amplitude. Finally, we can estimate the parameters of the GTD model by the proposed algorithm. This technique is robust with respect to noise and less than Nyquist sampling frequency. Another good property of the proposed method is its ability to handle closely spaced scattering centers that cannot be resolved by traditional methods.

The remainder of the paper is organized as follows. In Section 2, the GTD model of stepped-frequency radar target echoes is presented. Section 3 gives an overview of the CS principle, and Section 4 discusses the MCS algorithm and its application to parameter estimation in the GTD model. Simulation results are presented in Section 5, and Section 6 concludes this paper with a discussion of our work.

2. THE GTD MODEL OF RADAR TARGET ECHOES

Stepped-frequency waveforms can achieve high range resolution and do not require wide instantaneous bandwidth, which is widely used in modern radar systems. The improved range resolution of high-resolution radar or ISAR/SAR results in enhanced target detection and classification capability. Thus, we use the example of stepped-frequency radar in this paper. According to GTD theory, noisy radar target back-scattering data can be expressed as follows:

$$y(n)=\sum_{k=1}^{K} a_k\left(j\frac{f_n}{f_c}\right)^{\alpha_k}\exp\left[j\frac{4\pi f_n r_k}{c}\right]+w(n)\quad n=0,1,2,\ldots,N-1 \quad (1)$$

where the measurement noise $w(n)$ is Gaussian white noise and $f_n = f_c+n\Delta f$. f_c is the initial carrier frequency, N the number of pulses, Δf the frequency step, K the number of scattering centers in the model, a_k the scattering complex intensity of the kth scattering center, r_k the range of the kth scattering center with respect to a zero-phase reference, and α_k the geometric type parameter of the kth scattering center, which has the form $0.5l$ for $l \in \{-2,-1,0,1,2\}$. The five canonical scattering centers are summarized in Table 1.

For each localized scattering center, the aim of parameter estimation for the GTD model is to estimate the parameter set $\{K, a_k, \alpha_k, r_k\}$ $(k = 1,2,\ldots,K)$ according to the radar back-scattering data

Table 1. Type parameter for canonical scattering geometries.

Value of α	Example scattering geometries
-1	corner diffraction
$-1/2$	edge diffraction
0	point scatterer; doubly curved surface reflection; straight edge specular
$1/2$	singly curved surface reflection
1	flat plate at broadside; dihedral

received on a finite set of sampling frequencies. Note that the scattering centers of an actual target are located in very few positions over the whole region of interest (ROI) with stepped-frequency waveform high-resolution radar, and this provides the prerequisite condition that CS theory can be utilized for parameter estimation in the GTD model.

3. PRINCIPLES OF CS THEORY

CS theory [17, 18] is a new signal acquisition and reconstruction method that takes advantage of the sparsity or compressibility of signals. The algorithm originates from sparse signal decomposition and approximation theory, which can accomplish compressive sampling and recovery of initial signals based on the sparsity of signals, the randomness of the measurement matrix and the nonlinear optimization method. Different from Nyquist sampling, CS does not directly measure the signal itself, but projects it into low-dimensional space through a random measurement matrix. Thus, the measured data are the projection of signals from high to low-dimensional space [25]. Three essentials of CS are sparse transformation, incoherent measurement and nonlinear reconstruction, and the general concept is as follows.

Assume the initial signal $x_{N\times 1}$ is expressed as:

$$x_{N\times 1} = \sum_{i=1}^{N} \left\langle x, \varphi_i^T \right\rangle \varphi_i = \sum_{i=1}^{N} \beta_i \varphi_i \tag{2}$$

where $\langle \cdot, \cdot \rangle$ denotes the inner product, $(\cdot)^T$ the transpose, $\Psi = \{\varphi_i\}$, $(i = 1, 2, \ldots, N)$ the basis matrix, and $\beta = \{\beta_i\}$ are the projection coefficients of signals projected on Ψ. When β is a K-sparse signal (that is, only K of the coefficients are nonzero, while the other coefficients

are all zero or approximately zero, and $K \ll N$), $x_{N\times 1}$ is called a K-order sparse or compressible signal. As the power of a radar signal is finite, the square integrable signals $h(t)$ and $s(t)$ have the domain $[a, b]$. Thus,

$$\langle h(t), s(t)\rangle = \int_a^b h(t)s^*(t)dt \tag{3}$$

where $(\cdot)^*$ denotes the conjugate operation.

According to CS theory, the projection y is first obtained by projecting the original signal x on the measurement matrix $\Phi = \{\phi_i\}$, $(i = 1, 2, \ldots, M)$. β is then recovered from the measurement signal y. y can be expressed as

$$y_{M\times 1} = \sum_{i=1}^{M} \left\langle x, \phi_i^T \right\rangle \phi_i = \Phi_{M\times N}\Psi_{N\times N}\beta_{N\times 1} = \Theta\beta, \quad M < N. \tag{4}$$

In (4), an under-determined equation is needed to solve for β. From (2), we know that the reconstruction of x is equivalent to the reconstruction of β. According to CS theory, when the matrix multiplication $\Theta = \Phi\Psi$ satisfies the restricted isometry property (RIP) [13], K nonzero projective coefficients can be recovered, and the sample number must satisfy $M = O(K\log(N/K))$. The signal β can then be recovered from y by solving the following optimization problem:

$$\min\left(\|\beta\|_1\right) \quad \text{subject to} \quad y = \Phi\Psi\beta \tag{5}$$

The RIP implies that there exists $\delta_K \in (0, 1)$ such that

$$(1 - \delta_K)\|\beta\|_2 \le \|\Theta\beta\|_2 \le (1 + \delta_K)\|\beta\|_2$$

holds for an arbitrary K-sparse vector β. The smallest δ_K is the restricted isometry constant (RIC) of Θ. To recover the K-sparse vector β, δ_K should be smaller than 1. Many approaches can be used to reconstruct the K-sparse vector β satisfying (5), and the optimization problem can be efficiently solved by greedy algorithms such as matching pursuit [26], subspace pursuit [27], and orthogonal matched pursuit (OMP) [28]. An alternative solution is convex optimization [29], which is usually more precise but less efficient.

4. A NOVEL ALGORITHM FOR PARAMETER ESTIMATION FOR GTD MODEL

The following demonstrates the use of basic CS to estimate GTD parameters and a modified CS method for more accurate parameter estimation.

4.1. The CS Framework for Parameter Estimation in GTD Models

According to the above theory, the echo acquisition processing of stepped-frequency radar can be modeled as follows. Firstly, assume that there are S resolution cells in the observed scene, and the range to the zero-phase reference, back scattering coefficient, and parameter type of each scattering center is denoted as r_k, a_k, and α_k ($k = 1, 2, \ldots, K$), respectively. When the kth scattering center is located in resolution cell s_k, then $a(s_k) = a_k$, $\alpha(s_k) = \alpha_k$, and $r(s_k) = r_k$. If there is no scattering center in a resolution cell, the scattering coefficient or parameter type for that cell is zero. More importantly, the number of scattering centers of the radar target is much less than the number of resolution cells in the scene, which means the scene satisfies the sparsity condition.

We can write (1) in matrix form as

$$Y_{N\times 1} = \Psi'_{N\times S} I_{S\times 1} = \sum_k a_k \left(j\frac{f_n}{f_c}\right)^{\alpha_k} \exp\left[j4\pi f_n \frac{r_k}{c}\right] \tag{6}$$

where the column vector $\{\psi'_i\}$ of the basis matrix $\Psi'_{N\times S}$ satisfies:

$$\psi'_i = \left(\frac{f_n}{f_c}\right)^{\alpha(i)} \exp\left[j4\pi f_n \frac{r(i)}{c}\right] \quad i = 1, 2, \ldots, S \tag{7}$$

$$I_{S\times 1} = \left[a(1)j^{\alpha(1)}, a(2)j^{\alpha(2)}, \ldots, a(S)j^{\alpha(S)}\right]^T_{S\times 1} \tag{8}$$

In (7), the first segment is the amplitude modulation term of the basis matrix, when $f_c \gg N\Delta f$, $(f_n/f_c)^{\alpha(i)} \approx 1$, and its influence can be neglected under this condition. Equations (6)–(8) indicate that the original echo signal of the radar target can be linearly represented by a column vector of the basis matrix $\Psi'_{N\times S}$, and that the projective coefficient $I_{S\times 1}$, which is obtained by projecting the target echo signal onto $\Psi'_{N\times S}$, is a K-sparse vector.

As we must consider the influence of noise, the projective coefficient can be estimated as follows:

$$\min\left(\|I\|_1\right) \quad \text{subject to} \quad \left\|y - \Psi' I\right\|_2 < \varepsilon \tag{9}$$

where ε is the noise threshold, which can be estimated from noise-only range cells of the radar range profile. According to CS theory, there is always a random measurement matrix Φ that is utilized to enhance the orthogonality of $\Phi\Psi$, but this can rarely be used to improve the SNR of the measurement signal. Fortunately, a novel coherent accumulation matrix [30] can improve SNR whilst retaining the incoherence of $\Phi\Psi$.

Inspired by this, the estimation of $I_{S\times 1}$ by measurement signal $y_{N\times 1}$ can be expressed as:

$$\min\left(\left\|I'\right\|_1\right) \quad \text{subject to} \quad \left\|\Phi' y - \Phi'\Psi' W^{-1} I'\right\|_2 < \varepsilon' \tag{10}$$

where $\Phi'_{N\times N}$ is the Fast Fourier Transform matrix of N points, ε' the noise level after coherent accumulation, $I_{S\times 1} = W^{-1}_{S\times S} I'_{S\times 1}$, and the weighted matrix W is a diagonal matrix whose diagonal elements w_i represent weight values for the ith component of I. Unlikely the non-linear optimization methods based on Lagrange multiplier method to enhance radar imagery [33, 34]. The proposed modified compressive sensing algorithm enhances the reconstructed signal with partially known support as Equation (11) illustrates. Equation (11) is a convex problem and can be recast as a linear program [31], thus can be solved more efficiently than l_0-norm which is directly sparse restrict on I'. For Equation (11) is a convex problem, the solution of I' is a unique solution. On the other hand, Equation (11) can be treated as a linear program, so the solution of I' gets global convergence. Furthermore, as the number of acquired samples is increased under suitable conditions, this l_0-norm minimization is equivalent to an l_1-norm minimization and therefore faster to compute [17, 32].

In a previous study [30], $w_i = 1/|s_f(i)|$ and s_f is the Fourier Transform of y with zero-padding to give S points. As $|s_f(i)|$ is large, the weight of the ith component is considerable; thus, this weighting could lead to the analyzed signal concentrating on components with larger weight values. In such cases, the estimations exceed the true values of components with large weight values, while the estimations become smaller for those with small weight values. As far as the parameter estimation of scattering centers is concerned, the signal energy should focus on the target support region, where the weights of each component are supposed to be equal. Consequently, two different weight values are used in the proposed algorithm. The first is smaller and applied to range cells outside the target support region, whereas the second, larger weight value is applied within the target support region. Furthermore, the target support region can be determined by the noise threshold, which can be estimated from the range cells in which only noise exists. Once the noise threshold is obtained, the target support region is determined as the range cells in which noise exceeds the threshold. The diagonal elements of the weighted matrix can be expressed as

$$w_i = \begin{cases} 1/\max|s_f|, & |s_f(i)| > \lambda \\ 1/(\min|s_f| + v), & |s_f(i)| \le \lambda \end{cases} \tag{11}$$

where λ is the noise threshold, and the parameter $v > 0$ is introduced to satisfy the strict stability condition.

According to the above model, the projective coefficient $I_{S\times 1}$ can be estimated directly. Moreover, the positions of scattering centers can be estimated by searching the corresponding ranges for non-zero resolution cells of $I_{S\times 1}$. Assuming that the kth scattering center is located in the nth range cell, the GTD model parameters of the kth scattering center can be estimated as

$$r_k = r(n) \tag{12}$$

$$a_k = |I(n)| \tag{13}$$

$$\alpha_k = \text{angle}\,(I(n))/(\pi/2) \tag{14}$$

where $r(n) = r_0 + n\Delta r$, r_0 represents the distance of the first range cell, and Δr is the length of a range cell. Generally, Δr is less than $c/2N\Delta f$.

4.2. Parameter Estimation for GTD Model Based on Modified Compressed Sensing

Although CS theory can be utilized for parameter estimation in the GTD model, the position estimation values are discrete. However, in practical applications, the positions of target scattering centers are not strictly located at these discrete values. Furthermore, as the effect of noise is inevitable, the energy of a scattering center that has been projected to a sparse signal may be distributed in several (commonly two) neighboring cells. Thus, contiguous scattering cells should be combined, and a clustering methodology is applied to implement this process. When two neighboring resolution cells of $I_{S\times 1}$ are of the same type, the lower amplitude of the resolution cells is set to zero while the higher one is preserved. Because the clustering has been accomplished, the number of resolution cells with non-zero amplitude provides the estimated value of the target scattering center.

The sparse vector $I_{S\times 1}$ is reconstructed by (10), but the amplitude modulation term of the basis matrix Ψ' is ignored. This introduces some error into the amplitude estimation. As the energy of a single scattering center may spread over several scattering centers, some further error may be introduced to the intensity estimation of the scattering center. Hence, the least-minimum-squares algorithm is adopted to modify the amplitude of the scattering center. Thus, the position coordinate r and type parameter α of the scattering centers extracted by the proposed method can be obtained as above mention,

and the scattering intensity a can be calculated as:

$$a = \left(G^H G\right)^{-1} G^H y \tag{15}$$

$$G = [g(\alpha_1, r_1), g(\alpha_2, r_2), \ldots, g(\alpha_M, r_M)] \tag{16}$$

$$g(\alpha_i, r_i) = [(jf_0/f_c)^{\alpha_i} \exp\left(j4\pi f_0 r_i/c\right), (jf_1/f_c)^{\alpha_i} \exp(j4\pi f_1 r_i/c), \ldots, (jf_{N-1}/f_c)^{\alpha_i} \exp\left(j4\pi f_{N-1} r_i/c\right)]^T \tag{17}$$

In summary, the parameter estimation process for the GTD model is as illustrated in Fig. 1.

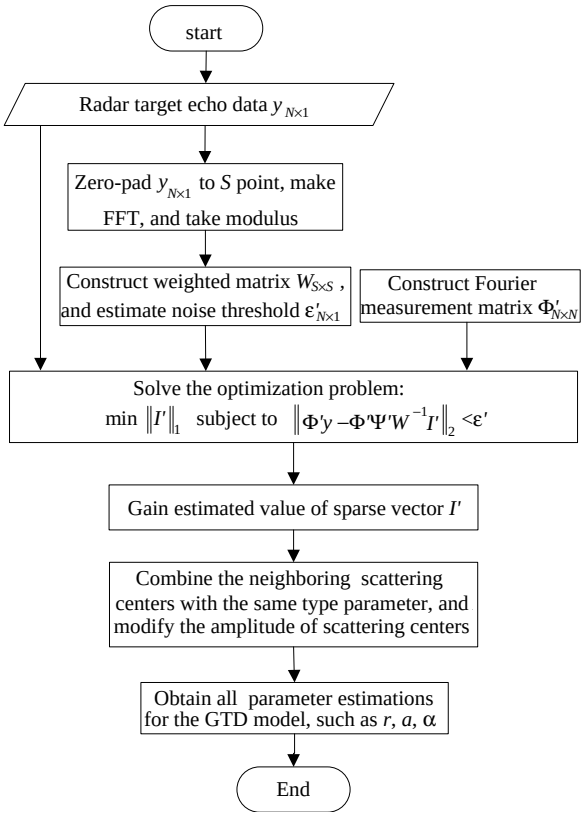

Figure 1. Flowchart of parameter estimation for GTD model.

5. SIMULATION EXPERIMENTS AND ANALYSIS

In this section, several examples are given to demonstrate the parameter estimation performance of our method compared with traditional spectrum estimation algorithms. First, we present an

example of parameter estimation using the proposed MCS algorithm and a target consisting of six point scatterers. We then compare the performance of MCS and three spectrum estimation algorithms under various SNR conditions and scatterers. The parameter estimations and reconstructed range profiles given by the MCS algorithm are contrasted with those from MUSIC, ESPRIT, and MEMP based on measured data.

5.1. Simulated Data

5.1.1. A Simple Example

We apply a stepped-frequency signal in all simulation experiments. The carrier frequency $f_c = 9\,\text{GHz}$, the frequency stepping number $N = 100$, and the frequency step $\Delta f = 2\,\text{MHz}$. Thus, the synthetic bandwidth of the radar is 200 MHz, and the corresponding range resolution based on traditional FFT is 0.75 m. Gaussian white noise is used for the receiver noise, and the measured target is formed from between five and eight ideal scatterer centers. Their specific parameters are listed in Table 2.

Setting the SNR to 10 dB and using six scattering centers (with indexes from 1–6) to form the target, there are $S = 256$ resolution cells in the measurement scenario (the region of interest is from −6.4–6.4 m). Therefore, based on the MCS algorithm, the range resolution is 0.05 m. Fig. 2(a) presents the reconstructed modulus value of $I_{S\times 1}$ under this scenario. The positions of the non-zero components of $I_{S\times 1}$ are almost consistent with the positions of the six scattering centers. However, a certain degree of error has been introduced as a result of noise and the energy of one scattering center spreading to neighboring resolution cells. In order to obtain more accurate results, the clustering and amplitude modification processes are adopted for scattering center estimation, and the final parameter estimations are illustrated in Figs. 2(b) and (c). As these results indicate, the proposed algorithm can effectively estimate the position, intensity, and types of all scattering centers of the target, even in noisy conditions.

Table 2. Parameters of target scattering centers.

Parameter \ Index	1	2	3	4	5	6	7	8
Position/m	−5	−2	−1	1	3	5	−6	6
Normalized Amplitude	0.707	0.5	0.707	0.5	0.707	1	1	0.5
Type	1	0.5	0.5	0	−1	−0.5	0	1

In order to illustrate the convergence of the proposed algorithm, 500 Monte Carlo experiments are made to gain the parameter estimation results for GTD model. All experiments obtain correct estimation results for all parameters of GTD model. In Fig. 3, the residual error of l_2 norm in Equation (10) is drawn via iterative number in convex optimization. The figure indicates that the error gets smaller as the iterative number adds. Though there is a minor error after 18th iterative, the reason is the existing noise. Further simulated results show that the error is reduced as the noise decreases, and I' can be exactly recovered when the noise vanishes.

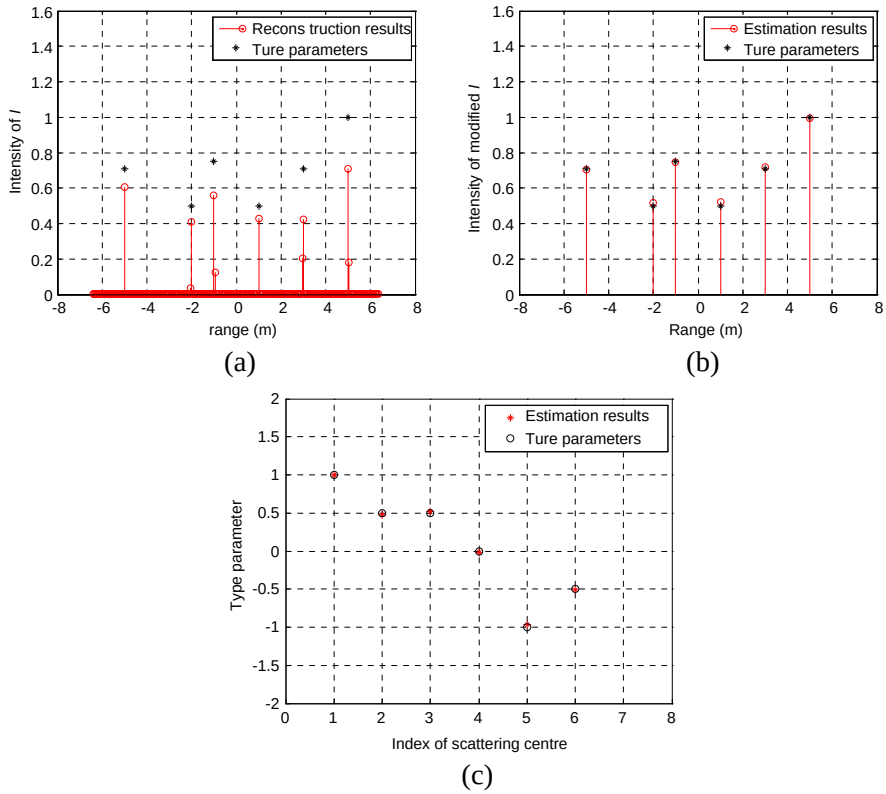

Figure 2. Parameter estimations by the proposed algorithm for GTD model. (a) True $|I_{S\times 1}|$ and estimation. (b) True positions, ranges, and their estimations. (c) True types and estimations.

5.1.2. Performance Comparison

To evaluate the proposed algorithm numerically, we conducted Monte Carlo simulations under several scenarios with different parameters. Furthermore, we compare the parameter estimation performance of our approach with that of three different spectrum algorithms, MUSIC, ESPRIT, and MEMP. This comparison consists of 1000 Monte Carlo simulations for each algorithm with different radar echo signals and different SNRs.

Two evaluation criteria are utilized for each algorithm: mean square error (MSE) and successful extraction probability (SEP). The MSE of the position parameter for a scattering center is defined as $\text{delta}(r) = \sqrt{E[(r - r')^2}$, where r is the real radial range of the scattering center, r' is the estimated value, and $E[\cdot]$ denotes the ensemble average. The MSEs of the other two parameters for the GTD model are defined similarly. The SEP is defined as the ratio of correct parameter estimations for all scattering centers to the total number of Monte Carlo simulations. Moreover, correct parameter estimation requires all scattering centers forming the target to be completely extracted and the MSEs of the range, amplitude, and type parameter of each scattering center to be below some preset threshold.

The MSEs of the parameter estimations for the GTD model with six scattering centers are illustrated in Fig. 4. As indicated by Figs. 4(a) and (b), all four algorithms obtain acceptable estimation results for the positions and amplitudes, exhibiting very low MSEs under high SNR conditions (SNR $>$ 12 dB). However, for lower SNRs (SNR $<$ 5 dB), MUSIC, ESPRIT, and MEMP obtain considerably worse estimation results. At low SNRs, the MCS algorithm exhibits

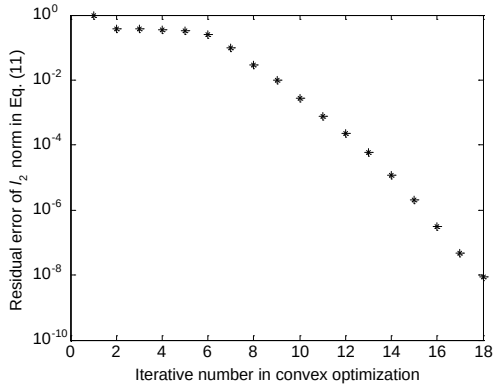

Figure 3. The convergence validation of proposed algorithm.

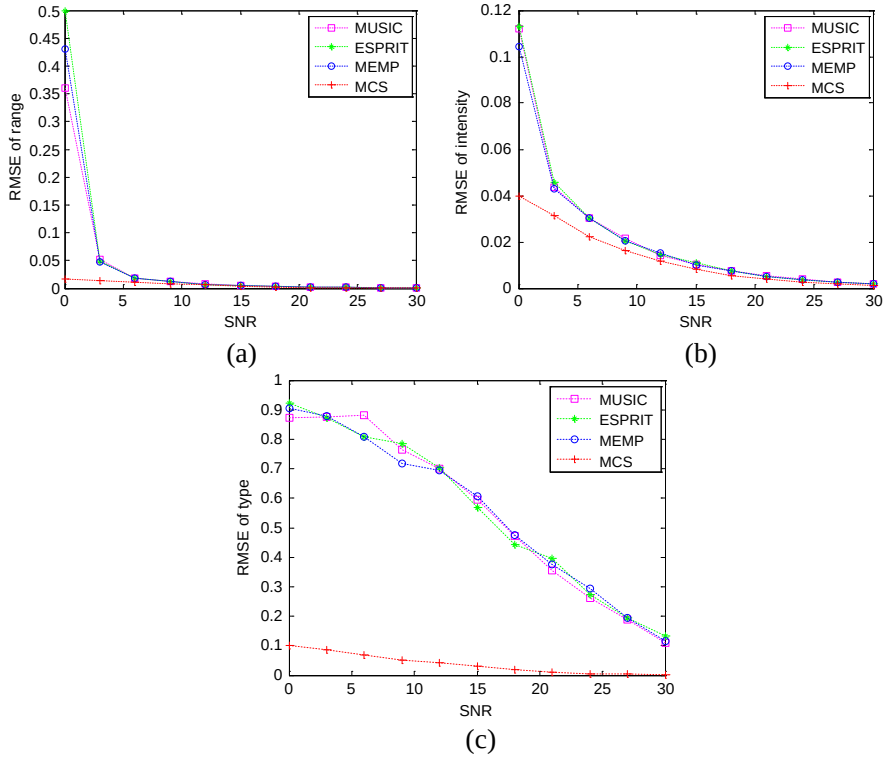

Figure 4. MSEs of parameter estimations for GTD model under different SNRs. (a) MSE of position estimation. (b) MSE of amplitude estimation. (c) MSE of type estimation.

better performance than the other three algorithms, with a smaller MSE. Fig. 4(c) illustrates the type parameter estimation results for all four algorithms. This indicates that the proposed MCS algorithm achieves better performance than the other spectrum estimation algorithms under all SNR conditions. More specifically, the MCS algorithm obtains more accurate type parameter estimation, with an MSE of less than 0.15 for SNRs in [0 dB, 30 dB], whereas the other spectrum estimation algorithms have MSEs for the type parameter of more than 0.35. From Figs. 4(a), (b), and (c), it can be seen that MCS achieves the best performance for all GTD model parameter estimations with SNRs in [0 dB, 30 dB], especially the type parameter estimation.

To allow further quantitative analysis of the scattering center extraction performance of the four algorithms, we calculated the SEP

with different numbers of scattering centers under different SNRs. The components of the radar target have five (index 1–5), six (index 1–6), seven (index 1–7), and eight (index 1–8) components, as shown in Table 2, and the SNR is in the range [0 dB, 12 dB]. If the relative MSE of all parameters for each scattering center is within 15% of the true value, the estimation results are considered to be correct. Moreover, as the estimation of the type parameter by the three spectrum estimation algorithms was considerably worse than the proposed MCS algorithm (Fig. 4(c)), this parameter is not considered in the SEP analysis. We conduct 1000 Monte Carlo simulations under each SNR with five, six, seven, or eight scattering centers. The simulation results are shown in Figs. 5(a), (b), and (c).

Several conclusions can be reached from these results. Firstly, from Fig. 5(a), we see that the SEP monotonically non-decrease relative to SNR for all four algorithms, reaching 100% for an SNR of 9 dB. This increasing trend is easy to understand, for as the noise get smaller, the target echo data achieves good consistency with the true GTD model, and thus all the algorithms obtain better performance. We can also see that the proposed MCS algorithm achieves a higher SEP than the other three spectrum estimation algorithms for SNRs below 9 dB.

Secondly, the SEP of the four algorithms is calculated for different numbers of scattering centers composing the radar target under an SNR of 5 dB. The results, as shown in Fig. 5(b), show that the SEP of all four algorithms decreases with an increase in K. This is because the complexity of the radar echo, which has a significant influence on the accuracy of parameter estimation, is closely related to K. Again, however, the proposed MCS method achieves the best performance of the four algorithms. There is a big gap between the SEPs of the MUSIC, ESPRIT, and MEMP algorithms and the proposed MCS algorithms with $K = 5$, but this gap shrinks as K increases.

Finally, Fig. 5(c) shows that the success estimation probability is a monotonic decreasing relative to SNR for all the four algorithms (i.e., MUSIC, ESPRIT, MPM and MCS). It is easy to understand this for as the noise get smaller, the target echo data achieves good consistency with the true GTD model, and thus all the algorithms obtain better performance. However, all of four algorithms have a lower success estimation probability as the K increases, and the reason is that the complexity of the radar echo enhance with K, which has great influence in the accuracy of parameter estimation.

In conclusion, it is obvious that the MCS algorithm can achieve outstanding performance compared to the modern spectrum estimation methods under different SNR condition. In addition, the

MCS algorithm obtains more accurate parameter estimation for the scattering centers when $K \leq 10$.

5.2. Measured Data in an Anechoic Chamber

We now measure the performance of our proposed MCS algorithm using real data from an anechoic chamber. The shape and geometrical size of a typical radar target is displayed in Figs. 6(a) and (b). Furthermore, the parameters of the stepped-frequency radar used for data acquisition are as follows.

The radar operates in the HH polarization state (i.e., the radar transmits and receives horizontal polarization), and the working frequency ranges from 8–12 GHz with a step size of 20 MHz. The

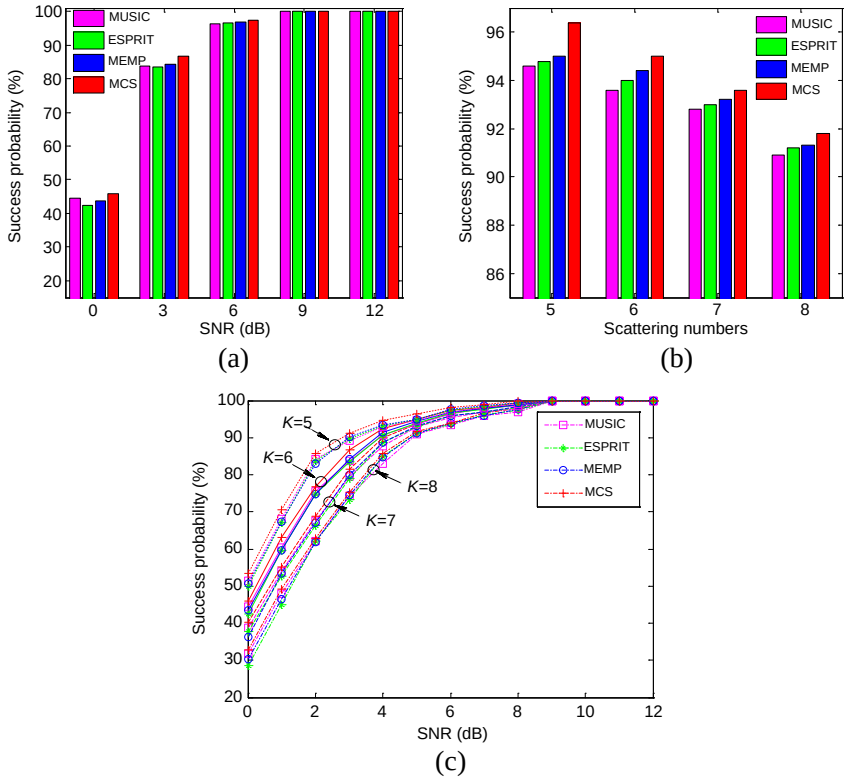

Figure 5. Successful estimation probability for different values of K and SNRs. (a) SEP vs. different SNRs (K= 6). (b) SEP vs. different K (SNR = 5). (c) SEP vs. different K and SNRs.

observation pitching angle is 0°, and the azimuth angle varies from 0–180° (0° corresponds to the no-sewing direction) with a step size of 0.2°. We measure data in the azimuthal range of 0–15° to validate the proposed MCS algorithm.

The parameter values estimated for the scattering centers by the MCS algorithm are illustrated in Fig. 7. These correspond to the 11th echo of the warhead and an azimuth angle of 2°. As Fig. 7 shows, the relative distance between the strong scattering centers are consistent with the geometry of the actual warhead model, and these centers are distributed on the head, the discontinuities in the middle and tail parts, and the two conical reflectors with small incident angles in the intermediate section. It should be pointed out that echoes from the scattering centers are sensitive to azimuth angle. Therefore, the number of scattering centers may vary with the azimuth angle. The measurement data show six scattering centers extracted for azimuth angles in [0°, 15°], which reflects the actual scattering centers of the warhead.

In order to compare the performance of MCS with the other three modern spectrum techniques, we conducted scattering center extractions and HRRP reconstructions using all four algorithms. The results are illustrated in Fig. 8. As this figure indicates, all algorithms are able to extract all six scattering centers on the warhead. However, the ESPRIT algorithm obtains a rather lower amplitude for the third scattering center. The other algorithms achieve a more reasonable amplitude estimation for all six scattering centers, although the proposed MCS algorithm reconstructs the most satisfactory HRRP, with the smallest MSE compared to the original HRRP. The actual parameter values and the estimates given by each algorithm are listed in Table 3 for all six scatterers on the warhead.

As Table 3 shows, for MUSIC, ESPRIT, and MEMP, some individual scattering center parameter estimates are close to their

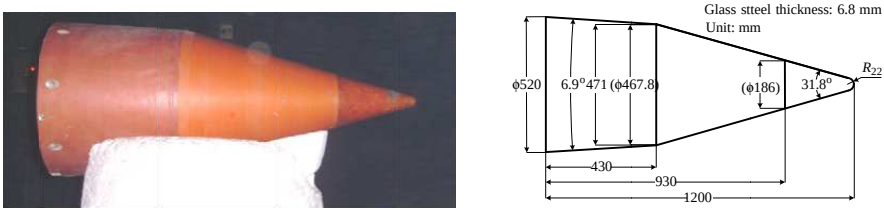

Figure 6. Actual shape and geometrical size of a scaled model of a warhead target. (a) Actual shape. (b) Geometrical size.

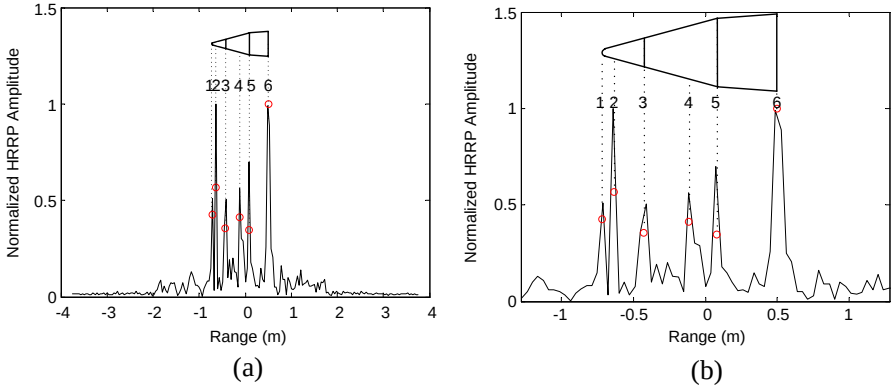

Figure 7. Scattering center extraction using the MCS algorithm. (a) Full domain. (b) Partial enlargement.

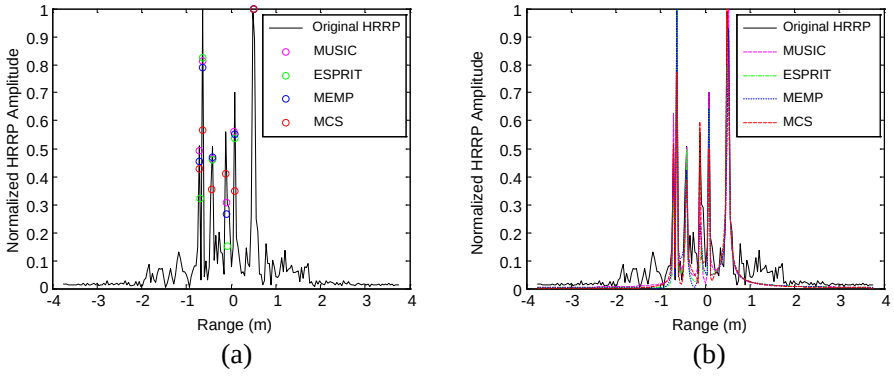

Figure 8. Scattering center extraction and HRRP reconstruction under azimuth angle of 2°. (a) Extracted scattering centers. (b) Reconstructed HRRP.

true value, whereas others are totally incorrect. On the other hand, the MCS algorithm obtains accurate type parameter estimations for all six scattering centers. Thus, we can state that the MCS algorithm exhibits outstanding performance in terms of type parameter estimation compared to the other three modern spectrum estimation algorithms.

We can analyze additional measured data to contrast the MCS algorithm with modern spectrum estimation algorithms. The 61st radar echo (corresponding to azimuth angle 12°) of the warhead gives the scattering centers shown in Fig. 9(a), and the reconstructed

HRRPs of all algorithms are illustrated in Fig. 9(b). This figure shows that the three modern spectrum estimation algorithms give mistaken range and amplitude estimations in one or two scattering centers, whereas the MCS algorithm estimates an acceptable range and amplitude for all six. Moreover, Fig. 9 also indicates that, when the measured data become inconsistent with the ideal GTD model, the modern spectrum estimation algorithms obtain rather poor range and amplitude estimation performance, while the MCS retains superior performance. Thus, the MCS algorithm provides more accurate parameter estimation and more extensive scope of application with actual measured data.

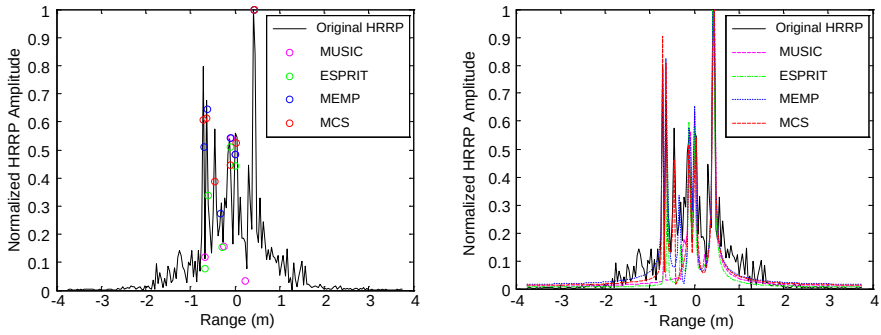

Figure 9. Scattering center extraction and HRRP reconstruction under azimuth angle of 12°. (a) Extracted scattering centers. (b) Reconstructed HRRP.

Table 3. Type parameter estimation of warhead scattering centers.

Parameter \ Index	1	2	3	4	5	6
Equivalent typical Geometry	point scatterer	flat plate at broadside	edge diffraction	flat plate at broadside	angle scatterer	edge diffraction
True type parameters	0	1	−0.5	1	−1	−0.5
MCS	0.106	0.964	−0.504	1.152	−1.08	−0.479
MUSIC	0.536	1.131	0.432	−0.536	−0.107	0.063
ESPRIT	−0.639	0.294	−0.519	0.495	1.235	0.675
MEMP	0.798	0.463	0.361	−0.043	−1.102	−0.987

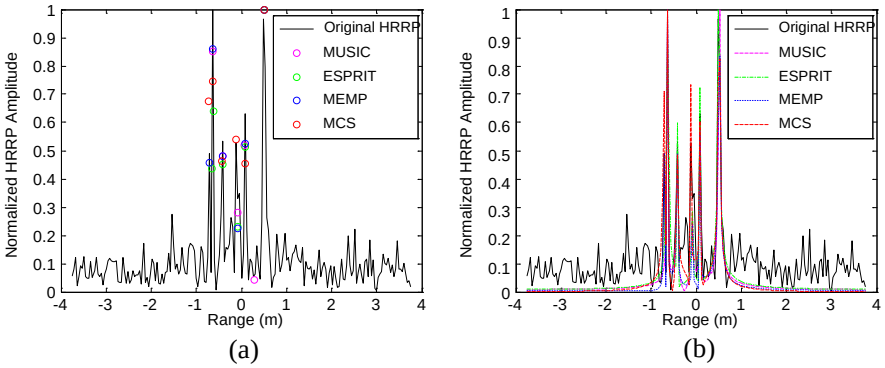

Figure 10. Scattering center extraction and HRRP reconstruction in noise condition. (a) Extracted scattering centers. (b) Reconstructed HRRP.

We now consider another two common conditions, namely the existence of noise and a decrease in sampling frequency. Specifically, Fig. 10 illustrates the scattering center extraction and HRRP reconstruction under the noise condition SNR = 30 dB at azimuth 2°. The MUSIC algorithm gives a false extraction of one scattering center, because it should only be applied for GTD parameter estimations with undamped harmonic signals. When the true target echo is significantly different from an undamped harmonic, the performance of this algorithm declines dramatically. In comparison, the ESPRIT and MEMP algorithms obtain slightly better estimation results, with some low amplitude estimates for one scattering center. However, the proposed MCS algorithm achieves outstanding performance. Moreover, Fig. 11 presents the extraction results and HRRP reconstruction with low sampling frequency (working frequency from 8–10 GHz) at azimuth 2°. This figure indicates that the MCS algorithm obtains more acceptable parameter estimation results than the MUSIC, ESPRIT, and MEMP algorithms. Additionally, the MCS algorithm gives range and amplitude estimations that are more consistent with the results of Fig. 10, whereas the modern estimation algorithms provide rather different results.

In conclusion, it is clear that the MCS algorithm can estimate the parameters of scattering centers more accurately than the modern spectrum estimation algorithms in different azimuth conditions, particularly the type parameter. We have shown that the MCS method is robust with respect to noise and a lower sampling frequency, a property not shared by the modern spectrum estimation algorithms.

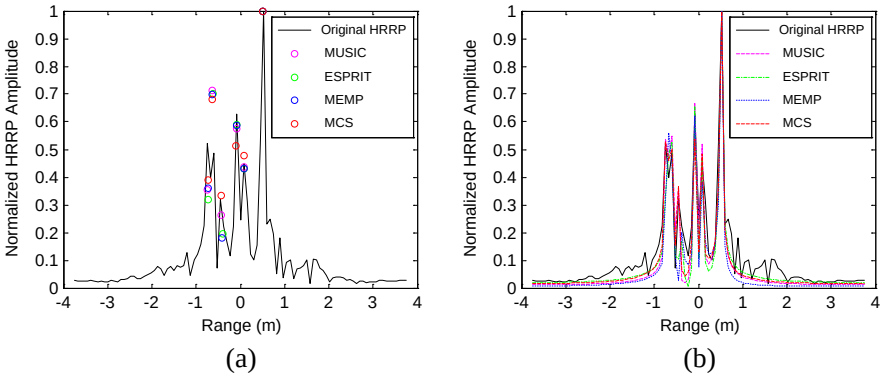

Figure 11. Scattering center extraction and HRRP reconstruction with low sampling frequency. (a) Extracted scattering centers. (b) Reconstructed HRRP.

6. CONCLUSIONS

Estimating radar target parameters for the GTD model is important in target recognition and other relevant areas. In this paper, we propose a novel parameter estimation algorithm for the GTD model. Our approach creatively adapts the theory behind Compressed Sensing. Firstly, we analyzed the sparseness of the amplitude and type vectors of target scattering centers along the range distribution. We then utilized an improved compressed sensing method to reconstruct the sparse vectors, modifying the data using clustering and least-minimum-squares. Finally, more accurate parameter estimations for the GTD model were obtained by the proposed MCS algorithm. In order to verify the effectiveness of MCS, we compared its performance with that of three different spectrum estimation algorithms using simulated and measured data via Monte Carlo experiments. The experimental results indicate that the MCS algorithm is significantly better than the comparative algorithms for all parameter estimations, especially the type parameter of the GTD model. Moreover, the proposed MCS method is more robust with respect to noise and lower sampling frequency, and obtains more accurate information about the scattering centers with measured data. Furthermore, the proposed MCS algorithm can be utilized in other waveform radar systems with a few adjustments, and has a variety of application areas.

REFERENCES

1. Keller, J. B., "Geometrical theory of diffraction," *J. Opt. Soc. Amer.*, Vol. 52, No. 2, 116–130, Jan. 1962.
2. Tseng, N. and W. D. Burnside, "A very efficient RCS data compression and reconstruction technique," Tech. Rep. No. 722780-4, ElectroSci. Lab, Ohio State University, Columbus, 1992.
3. Wang, Y. and H. Ling, "A model-based angular extrapolation technique for iterative method-of-moments solvers," *Microwave and Optical Technology Letters*, Vol. 20, No. 4, 229–233, Feb. 1999.
4. Gupta, I. J., M. J. Beals, and A. Moghaddar, "Data extrapolation for high resolution radar imaging," *IEEE Transactions on Antennas and Propagation*, Vol. 42, No. 11, 1540–1545, Nov. 1994.
5. Zhang, X., J. Qin, and G. Li, "SAR target classification using Bayesian compressive sensing with scattering centers features," *Progress In Electromagnetics Research*, Vol. 136, 385–407, 2013.
6. Kim, K.-T. and H.-T. Kim, "One-dimensional scattering centre extraction for efficient radar target classification," *IEE Proc. — Radar, Sonar and Navigation*, Vol. 146, No. 3. 147–158, Jun. 1999.
7. Sdeedly, W. M. and R. L. Moses, "High resolution exponential modeling of fully polarized radar returns," *IEEE Transactions on Aerospace and Electronic Systems*, Vol. 27, No. 3, 459–469, May 1991.
8. McClure, M., R. C. Qiu, and L. Carin, "On the superresolution identification of observables from swept-frequency scattering data," *IEEE Transactions on Antennas Propagations*, Vol. 45, No. 4, 631–641, Apr. 1997.
9. Potter, L. C., D.-M. Chiang, R. Carriére, and M. J. Gerry, "A GTD-based parametric model for radar scattering," *IEEE Transactions on Antennas and Propagations*, Vol. 43, No. 10, 1058–1067, Oct. 1995.
10. Bo, H. Y., "Estimating two-dimensional frequencies by matrix enhancement and matrix pencil," *IEEE Transactions on Signal Processing*, Vol. 40, No. 9, 2267–2280, Sep. 1992.
11. Chen, F. J. and C. Carrson, "Estimation of two-dimensional frequencies using modified matrix pencil method," *IEEE Transactions on Signal Processing*, Vol. 55, No. 2, 718–724, Jan. 2007.
12. Schmidt, R. O., "Multiple emitter location and signal parameter estimation," *IEEE Transactions on Antennas Propagations*, Vol. 34, No. 3, 276–280, Mar. 1986.

13. Jiang, J., F. Duan, and J. Chen, "Three-dimensional localization algorithm for mixed near-field and far-field sources based on ESPRIT and MUSIC method," *Progress In Electromagnetics Research*, Vol. 136, 435–456, 2013.
14. Roy, R. and T. Kailath, "ESPRIT-estimation of signal parameters via rotational invariance techniques," *IEEE Transactions on Acoustics, Speech and Signal Processing*, Vol. 37, No. 7, 984–995, Jul. 1989.
15. Stoica, P. and Y. Selen, "Model-order selection: A review of information criterion rules," *IEEE Signal Processing Magazine*, Vol. 21, No. 4, 36–47, Jul. 2004.
16. Donoho, D., "Compress sensing," *IEEE Trans. Inf. Theory*, Vol. 52, No. 4, 1289–1306, Apr. 2006.
17. Candés, E., J. Romberg, and T. Tao, "Robust uncertainty principle: Exact signal reconstruction from highly incomplete frequency information," *IEEE Trans. Inf. Theory*, Vol. 52, No. 2, 489–509, Feb. 2006.
18. Liu, Z., X. Z. Wei, and X. Li, "Adaptive clutter suppression for airborne random pulse repetition interval radar based on compressed sensing," *Progress In Electromagnetics Research*, Vol. 128, 291–311, 2012.
19. Herman, M. and T. Strohmer, "High-resolution radar via compressive sensing," *IEEE Transactions on Signal Processing*, Vol. 57, No. 6, 2275–2284, Jun. 2009
20. Gurbuz, A. C., J. H. McClellan, and W. R. Scott, "A compressive sensing data acquisition and imaging method for stepped frequency GPRs," *IEEE Transactions on Signal Processing*, Vol. 57, No. 7, 2640–2650, Jul. 2009.
21. Huang, Q., L. Qu, B. Wu, and G. Fang, "UWB through-wall imaging based on compressive sensing," *IEEE Trans. Geosci. Remote Sens.*, Vol. 48, No. 3, 1408–1415, Mar. 2010.
22. Li, J., S. S. Zhang, and J. F. Chang, "Applications of compressed sensing for multiple transmitters multiple azimuth beams SAR imaging," *Progress In Electromagnetics Research*, Vol. 127, 259–275, 2012.
23. Wei, S.-J., X.-L. Zhang, J. Shi, and G. Xiang, "Sparse reconstruction for SAR imaging based on compressed sensing," *Progress In Electromagnetics Research*, Vol. 109, 63–81, 2010.
24. Zhang, L., M. Xing, C. Qiu, et al., "Achieving higher resolution ISAR imaging with limited pulses via compressed sampling," *IEEE Geoscience and Remote Sensing Letters*, Vol. 6, No. 3, 567–

571, Jun. 2009.

25. Baraniuk, R. G., "A lecture on compressive sensing," *IEEE Signal Processing Magazine*, Vol. 24, No. 4, 118–12l, Jul. 2007.
26. Mallat, S. and Z. Zhang, "Matching pursuit with time-frequency dictionaries," *IEEE Transactions on Signal Processing*, Vol. 41, No. 12, 3397–3415, Dec. 1993.
27. Dai W. and O. Milenkovic, "Subspace pursuit for compressive sensing signal reconstruction," *IEEE Trans. Inf. Theory*, Vol. 55, No. 5, 2230–2249, May 2009.
28. Tropp, J. A. and A. C. Gilbert, "Signal recovery from random measurements via orthogonal matching pursuit," *IEEE Trans. Inf. Theory*, Vol. 53, No. 12, 4655–4666, Dec. 2007.
29. Grant, M. and S. Boyd, CVX: Matlab Software for Disciplined Convex Programming (Web Page and Software), 2011, Available: http://stanford.edu/ boyd/cvx.
30. Zhang, L., M. Xing, C. Qiu, et al., "Resolution enhancement for inversed synthetic aperture radar imaging under low SNR via improved compressive sensing," *IEEE Trans. Geosci. Remote Sens.*, Vol. 48, No. 10, 3824–3838, Oct. 2010.
31. Wang, M. and W. Xu, "On the performance of sparse recovery via l_p-minimization $(0 \leq p \leq 1)$," *IEEE Trans. Inf. Theory*, Vol. 57, No. 10, 7255–7278, Oct. 2011.
32. Candès, E. J. and T. Tao, "Decoding by linear programming," *IEEE. Trans. Inf. Theory*, Vol. 51, No. 12, 4203–4215, Dec. 2005.
33. Browne, K. E. and R. J. Burkholder, "Non-linear optimization of through-wall radar images via the lagrange multiplier method," *IEEE Geoscience and Remote Sensing Letters*, Vol. 9, No. 5, 803–807, Sep. 2012.
34. Burkholder, R. J., A. N. O'Donnell, W. O. Coburn, and C. J. Reddy, "Sparse basis expansion for compressive sensing of electromagnetic scattering patterns computed using iterative physical optics," *2012 International Conference on Electromagnetics in Advanced Applications (ICEAA 2012)*, Cape Town, South Africa, Sep. 2–7, 2012.